Isothermal Crystallizaiton Kinetic and Melting Behaviors of Nylon 6/66/510

Lei Zhou[1], Weilan Xue[1*] and Zuoxiang Zeng[1]

[1]*Institute of Chemical Engineering, East China University of Science and Technology, 200237 Shanghai, China.*

Authors' contributions

This work was carried out in collaboration between all authors. Author LZ designed the study, performed the analytical studies and wrote the first draft of the manuscript. Author WX managed the analyses of the study. Author ZZ revised the manuscript. All authors read and approved the final manuscript.

Article Information

Original Research Article

ABSTRACT

In this work, nylon 6/66 (S0) and nylon 6/66/510 (S1~S3) containing 5 ~ 15 mol % nylon-510 were synthesized by melt condensation polymerization and the isothermal crystallization kinetics and melting behaviors after isothermal crystallization of copolymer were systematically studied by differential scanning calorimetry (DSC). The chemical structures and molecular weights were characterized by means of nuclear magnetic resonance (^{1}H-NMR). The values of $t_{1/2}$ and the equilibrium melting temperature for all samples were calculated by Avrami equation and Hoffman-Weeks, respectively. The crystal structure of the copolyamides were also investigated by wide-angle X-ray diffraction (WARD). The results shows that: (1) Avrami model can be used to well describe the isothermal crystallization behavior of the copolyamides, and all the values of $t_{1/2}$ increase with increasing the T_c or the mole fraction of nylon 510. (2) The crystallization activation energy (ΔE) and nucleation constant (K_g) both increase with increasing the mole fraction of nylon-510, which indicating that the addition of nylon nylon-510 decreases the crystallization rate of copolymer.

_____

Corresponding author: E-mail: wlxue@ecust.edu.cn;

1. INTRODUCTION

Nylon, exhibiting a high modules, toughness and strength, low creep and good temperature resistance, is used in automobile industries, electricity-related areas, and electronics [1]. Among various types of copolyamides, Nylon 6 and Nylon 66 are the most widely studied [2-5]. Gehard Poessnecker et al. [6] synthesized a coplyamide nylon 6/66/1010, which displays low melting point, good mechanical property and excellent heat resistance. The obtained nylon 6/66/1010 was successfully applied in the fibers films. Additionally, Xiaolin Xiao et al. [7] reported the isothermal crystallization kinetic and melting behaviors of poly(butylene terephthalate) and poly (butylenes terephthalate-co-fumarate) copolymer and found that the introduction of fumarate into PBT chains attenuated the crystallization rate of PBT in PBTF [8]. Moreover, Syang-Peng et al. [9] researched the crystallization kinetics of nylon6/6T and nylon 66/6T copolymer. However, previous studies mainly focused on the synthesis and thermal properties, there is little information about the isothermal crystallization of terpolymer [10-13]. On the other hand, the physichemical and mechanical properties of nylon deeply depended on their crystallization structure. Therefore, it was important to investigate the crystallization kinetics.

In this study, a novel copolyamides, nylon 6/66/510, was synthesized by the method of melting condensation polymerization. The isothermal crystallization kinetics and melting behaviors after isothermal crystallization of copolymer were systematically studied by differential scanning calorimetry (DSC). The chemical structures and molecular weights were characterized by means of nuclear magnetic resonance (^{1}H-NMR). The values of $t_{1/2}$ and the equilibrium melting temperature for all samples were calculated by Avrami equation and Hoffman-Weeks, respectively. The crystal structure of the copolyamides were also investigated by wide-angle X-ray diffraction (WARD).

2. EXPERIMENTAL

2.1 Materials

Caprolactam was obtained from Zhejiang Quzhou JuHua Nylon Co. Ltd. (China); nylon 66 salt was purchased from BASF Company Ltd. (China); 1,5-pentanediamine sebacic acid was supplied by Zhejiang Yisheng petrochemical Co., Ltd; stearic acid was used as the capping agent and supplied by Acidchem International Sdn. Bhd (Malaysia).

2.2 Preparation of Copolyamide

Five samples of copolyamies were prepared by condensation of caprolactam, nylon 66 salt, and nylon-510 salt. The X_m (the mole fraction of nylon-510) value was calculated based on the added amounts of 1,5-pentanediamine and sebacic acid. Formulas for the preparation of the copolyamides are shown in Table 1. To start the reaction, caprolactam, nylon 66 salt, 1,5-pentanediamine and sebacic acid were put into an autoclave and heated to 250℃. The pressure was maintained at 1.6 MPa for 1.5 h. Then the pressure is slowly reduced to atmospheric pressure, and the polymerization was carried out under the pressure for another 1.5 h at 250℃. The obtained product was taken out of autoclave and allowed to cool at room temperature. The obtained nylon 6/66 and nylon 6/66/510 with different mole fraction (5, 10 and 15 mol%) were denoted as S0, S1, S2 and S3 respectively.

2.3 Characterization

2.3.1 Nuclear magnetic resonance (^{1}H-NMR) analysis

^{1}H-NMR was measured using a Bruker Avance-500 MHz spectrometer at room temperature. (CF$_3$)$_2$CDOD was used as the solvent, and all the samples were purified before measurement.

Table 1. The quantities of raw material added and mole fraction of nylon-510

Material	S0	S1	S2	S3
Caprolactam (mol)	1.929	1.929	1.929	1.929
Nylon-66 salt (mol)	0.769	0.769	0.769	0.769
1,5-pentanediamine (mol)	-	0.144	0.302	0.478
Sebacic acid(mol)	-	0.142	0.300	0.476
X_m (mol%)	0	5	10	15

2.3.2 Gel permeation chromatography (GPC)

The average weights (M_n, M_w) of the polyamides were determined by Waters 1515 Gel Permeation Chromatography (GPC) at 25℃. The elution times and RI detector were calibrated with a commercial calibration polysaccharide.

2.3.3 Differential scanning calorimetry (DSC)

The differential scanning calorimetry (DSC, METTLER TOLEDO, Switzerland) was used to measure the isothermal crystallization kinetics and the glass transition temperature (T_g). All DSC tests were carried out in the temperature range from -20℃ to 250℃ at a heating rate of 10℃/min under nitrogen atmosphere. Samples of about 5 mg were put into aluminium pan for DSC measurements. Before DSC tests, all samples were heated rapidly (60℃/min) to 200℃ and kept for 5 min and then cooled (-70℃/min) to the desired temperature.

2.3.4 Wide-angle X-ray diffraction (WAXD)

X-Ray Diffraction (XRD) data was collected at room temperature using a BRUKER-AXC08 X-ray diffractometer (Cu Kα radiation, λ=0.1542 nm, voltage 40 KV, 100mA, USA). The samples of P0-P4 were scanned from 3 to 50° 2 θ with a step size of 0.02°.

3. RESULTS AND DISCUSSION

3.1 Chemical Structures

The chemical structure of prepared copolyamides was confirmed by ^{1}H-NMR using $(CF_3)_2CDOD$ as solvent, and the ^{1}H-NMR spectra of S3 is illustrated in Fig. 1. As can be seen, the characteristic peaks of S3 show proton resonances at 3.00, 7.71, and 1.33 ppm, which can be assigned to the protons in –NH-C=O (from caprolactam), -CH2- (from nylon-510), –NH-C=O (from nylon66), respectively [9]. What is more, according to the heights of characteristic peaks, the molar ratio of caprolactam, nylon-510 to nylon-66 caprolactam is close to 5:1:2, which is consistent with the raw material ratio of S3 [10].

3.2 The Molecular Weights

The molecular weights (M_n, M_w) of S0~S3 were measured by the procedure described in Section 2.3.2, and the results were summarized in

Table 2. As shown in Table 2, the M_w value of the samples was basically stable and ranged from 66,000 to 57,000Da. On the other hand, the molecular weight distribution (M_w/M_n) of copolyamides was increased from 1.18 to 1.38 when the X_m value was increased from 0 to 15 mol %.

Table 2. Molecular weights measured by GPC

	S0	S1	S2	S3
M_w(Da)	66,000	57,000	59,000	65,000
M_n (Da)	55,900	46,300	45,000	47,000
M_w/M_n	1.18	1.23	1.31	1.38

3.3 Melting Behavior and Equilibrium Melting Temperature

The DSC heating scans for S0~S3 after isothermal crystallization at indicated temperature were measured by the procedure described in Section 2.3.2, and the results were summarized in Fig. 2 and Table 3. From the results, two melting endothems of these samples were displayed for all samples. Moreover, the first melting peak [referred as $T_m(I)$] shifts to a higher temperature with increasing T_c, while the second melting endothem position [referred as $T_m(II)$] is independent on T_c. The double melting behaviors of this polymers can be ascribed to recrystallization phenomena during the heating process [11]. Thus, the $T_m(I)$, related to the fusion of crystals grown at T_c, is defined as melting point (T_m) and used for the determination of equilibrium melting temperature (T_m^0). With increasing T_c, the crystals become more perfect and $T_m(I)$ is is enhanced. The second melting peak is attributed to the melting of crystallite formed by melting and recrystallization during the DSC heating scanning [11].

The equilibrium melting temperature (T_m^0), an important parameter characteristic of the crystal of the liner polymer, can be determined by the plot of the experimental T_m - T_c data using the Hoffman-Weeks equation [14].

$$T_m = T_m^0(1-1/\beta)+T_c/\beta \qquad (1)$$

Where β is a factor depending on the lamellar thickness and $\beta=l/l_0$, where l and l_0 are the thicknesses of mature crystallite and of the critical crystalline nucleus. T_c and T_m are the crystallization and melting temperature, respectively.
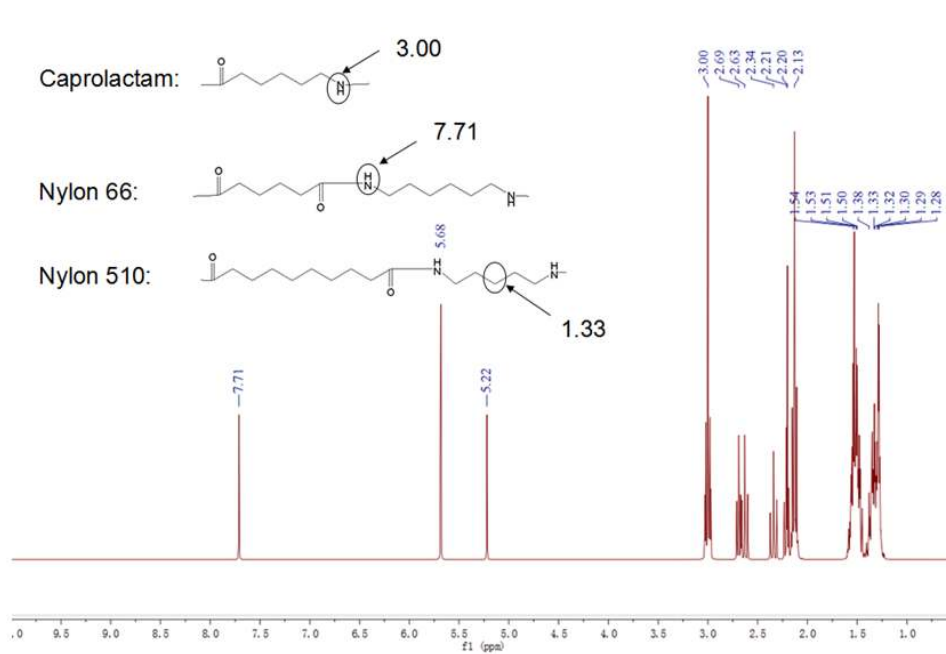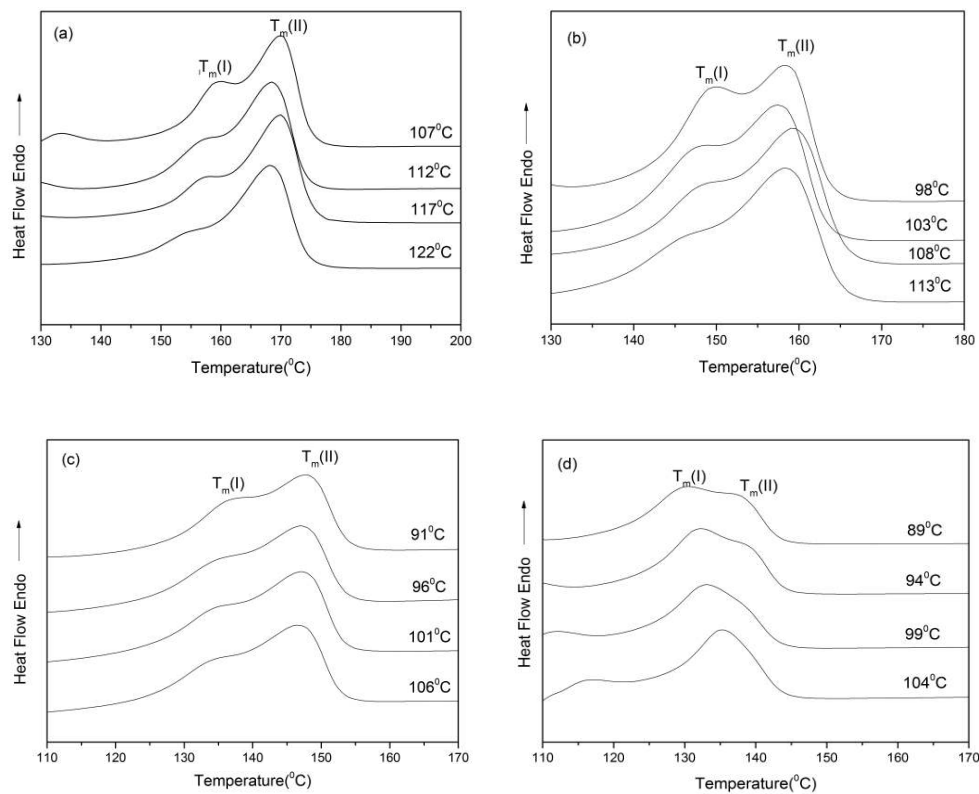
3

Fig. 1. ^{1}H-NMR spectra of sample S3

Fig. 2. The DSC curves of samples at a heating rate of 10℃/min: (a) S0; (b) S1; (c) S2; (d) S3

From Table 3 and Fig. 3, it can been seen that decreases with increasing the mole fraction of nylon-510, which is attributed to the change of molecular structure of samples [15].
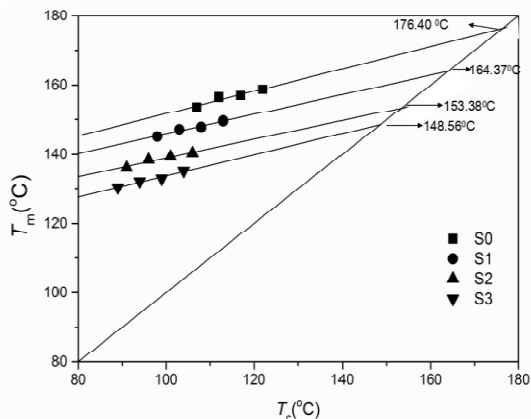

Fig. 3. The melting temperature of Tm(I) taken as a function of the crystallization temperature for S0, S1, S2, and S3

3.4 Isothermal Crystallization Kinetics Base on Avrami Equation

The crystallization kinetics for copolyamide was characterized using isothermal method. Fig. 4 shows the representative isothermal crystallization DSC traces for S0 and S2 at different temperature. Based on the results in Fig. 4, the crystallization peaks show right shifts and become flatter with increasing crystallization temperature. It meant that the sample with higher

crystallization temperature requires a longer time to complete crystallization.

The isothermal crystallization process can be expressed by Avrami equation as shown in the following [16,17]:

$$X(t) = 1 - \exp(-Kt^n) \qquad (2)$$

$$\log\{-\ln[1 - X(t)]\} = n\log t + \log K \qquad (3)$$

Where $X(t)$, the relative crystallinity, is defined as the ratio of crystallinity developed at time t to crystallinity developed at time t→∞.Where K is the isothermal crystallization rate parameter; n was the Avrami exponent which is related to nucleation mechanisms and the dimensions of the growth during the crystallization. $X(t)$ can be obtained by the following equation [16]:

$$X(t) = \frac{\Delta H_t}{\Delta H_0} = \frac{\int_0^t \frac{dH}{dt} dt}{\int_0^\infty \frac{dH}{dt} dt} \qquad (4)$$

Where ΔH_t is defined as the total heat evolved at time t; ΔH_0 is defined as the total heat evolved as time approaches infinity. Fig. 5 shows the relationship between relative crystallization ($X(t)$) and crystallization time at different crystallization temperature. From the results showed in Fig. 5, the isothermal crystallization curve shift to the right with the increase of crystallization temperature, which indicates the crystallization rate decreased.

Table 3. Melting parameters of crystalline polymers

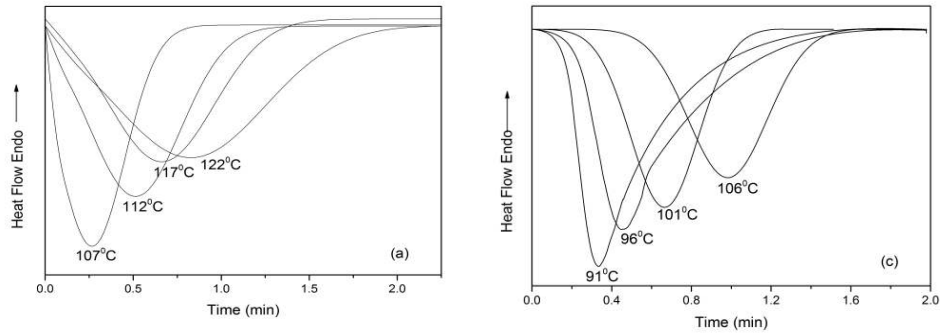| Polymer	T_c (°C)	$T_m(I)$ (or T_m) (°C)	$T_m(II)$ (°C)	$T0$ m (°C)
S0	107	153.50	168.35	176.40
	112	156.47	168.55	
	117	157.01	169.86	
	122	158.70	170.06	
S1	98	145.14	158.33	164.37
	103	147.17	159.41	
	108	147.82	158.48	
	113	149.64	158.25	
S2	91	136.06	146.58	153.38
	96	138.42	147.10	
	101	139.33	147.11	
	106	140.27	147.65	
S4	89	130.38	138.07	148.56
	94	132.14	139.11	
	99	132.97	138.66	
	104	135.21	139.22	

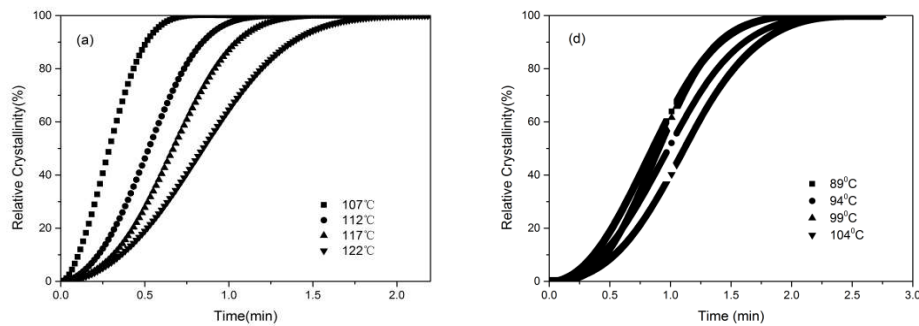**Fig. 4. The DSC curves of (a) S0 and (c) S2**

Fig. 5. The development of relative crystallinity with time at different crystallization temperatures: (a) S0 and (d) S3

Fig. 6 shows the plots of log{-ln[1-$X(t)$]} versus log$t$ for S0 and S1. Similar relationship curves are also obtained for S2 and S3. From Fig. 6, the Avrami exponent n and K are obtained from the slop and intercept and listed in Table 4. As seen in Table 4, the n values range from 1.74 to 2.80, which indicates that the copolyamides contain the homogeneous nucleation and heterogeneous nucleation at the same time. On the other hand, the K values of copolyamides decrease with the

increase of T_c for each sample, which indicates the higher crystallization temperature, the slower the homogeneous nucleation [18,19].

Crystallization half-time, $t_{1/2}$, is another important crystallization kinetic parameter. It is defined as the time at which crystallization is 50%. Crystallization half-time, which can be obtained from Fig. 5, can also be calculated from the following equations [16,17]:
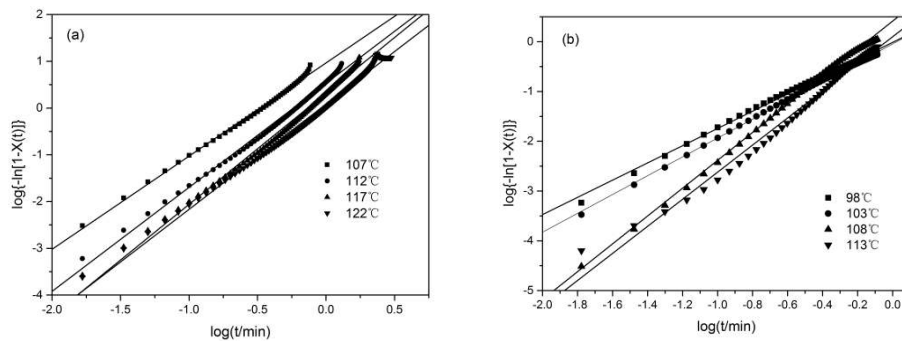

Fig. 6. Avrami Polts of log{-ln[1-$X(t)$]} versus *logt* at different crystallization temperatures: (a) S0 and (b) S1

6

$$t_{1/2} = (\ln 2 / K)^{1/n} \qquad (5)$$

$$\delta = \frac{|t_{1/2} - \tau_{1/2}|}{t_{1/2}} \qquad (6)$$

As seen from Table 4, all the values of $t_{1/2}$ increase with increasing the T_c or the mole fraction of nylon-510, which means the slower cystallization rate. What's more, the values of $t_{1/2}$ at different T_c calculated from Eq. 5 are close to the experiment value(where $\varepsilon_{1/2}$ stand for the $t_{1/2}$ obtained form Fig. 5 and δ stand for the deviation of $t_{1/2}$), which means that the Avrami model can be used to describe the isothermal crystallization of the copolyamide.

3.5 Crystallization Activation Energy (ΔE)

The crystallization process of copolyamides is assumed to be thermally activated, the following Arrhenius equation can be used to described the crystallization rate parameter K [17].

$$K^{1/n} = k_0 \exp(\frac{-\Delta E}{RT_c}) \qquad (7)$$

$$\frac{1}{n} \ln K = \ln k_0 - \frac{\Delta E}{RT_c} \qquad (8)$$

Where ΔE is defined as the crystallization activation energy, R is the universal gas constant. Fig. 7 shows the plots of $(1/n)\ln K$ versus $1/T_c$ for S0, S1, S2, and S3, which has a good linear relationship. The values of ΔE are -676.24, -471.99, -248.84, and -243.69 kJ/mol for S0, S1, S2, and S3, respectively. The values of ΔE increase with the increasing the mole fraction of nylon-510, which is because the incorporation of new comonomer disturbs the regularity and reduces the crystallization order [14,20].

3.6 Spherulite Growth Based on Lauritzen-Hoffman Equation

The classic Lauritzen-Hoffman equation is adopted to describe the crystallization of a polymer in terms of the kinetics and thermodynamics of polymer surface nucleation and the spherulite growth rate in the isothermal crystallization process of the homopolymer and copolymers for higher degrees of supercooling [10]. The overall crystallization rate G, is defined as the reciprocal of $t_{1/2}$, should not be interpreted

as simple spherulitic radial growth because of the combination of nucleation and growth phenomena [11]. The temperature dependence of the linear growth rate G is given by the relationship:

$$G = G_0 \exp[\frac{-U^*}{R(T_C - T_\infty)}] \exp[\frac{-K_g}{fT_c \Delta T}] \qquad (9)$$

Where G_0 is a pre-expontential factor, $\overset{*}{U}$ is the transport activation energy, which is associated with the molecular diffusion across the interfacial boundary between melt and crystals. T_∞ is the hypothetical temperature and K_g is a nucleation parameter [12], $f = 2T_c / (T_m^0 + T_c)$ is a correction factor and $\Delta T = T0$ m.-T_c. The growth rate G can be replaced by the half time of crystallizaion $t_{1/2}$. So the Equation 9 can also be written as follows:

$$\ln(1/t_{1/2}) + \frac{U^*}{R(T_c - T_\infty)} = \ln G_0 - \frac{K_g}{fT_c \Delta T} \qquad (10)$$

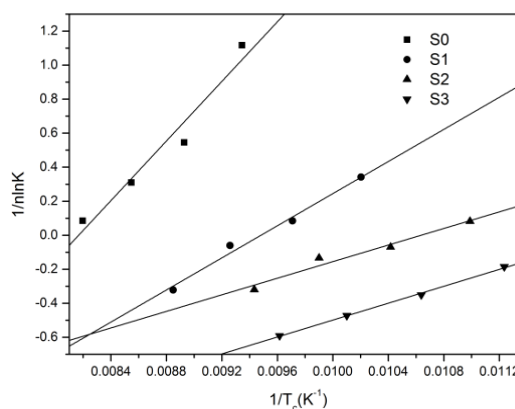Hoffman et al. Found $\overset{*}{U} = 1500$ cal/mol and $T_\infty = (T_g - 30)$K.

Fig. 7. The plots of the Avrami parameters $(1/n)\ln K$ versus $1/T_c$ for the acquisition of the isothermal crystallization activation energy for S0, S1, S2, and S3

As can been seen from Fig. 8, the plots of $\ln G + \overset{*}{U}/[R(T_c - T_\infty)]$ versus $1/[fT_c \Delta T]$ are approximately linear for all samples, indicating that the Lauritzen-Hoffman equation can well describe the crystallization process of the homopolymer and copolymer. The values of K_g and G_0 can be obtained from the slope and intercept of Fig. 8, respectively. The results shows that S0 has a higher values than that of S1, S2, and S3, which

Table 4. Kinetic parameters for the isothermal crystallization of copolyamide

Sample	T_c (℃)	n	K (min^{-n})	R^2	$t_{1/2}$(min)	$\varepsilon_{1/2}$(min)	δ(%)
P0	107	1.99	9.22	0.9957	0.29	0.27	6.04
	112	2.23	3.37	0.9943	0.52	0.49	5.84
	117	2.37	2.08	0.9937	0.67	0.63	6.16
	122	2.24	1.21	0.9931	0.85	0.78	7.79
P1	98	2.80	2.60	0.9951	0.62	0.62	0.01
	103	2.72	1.26	0.9936	0.77	0.80	4.77
	108	1.74	0.90	0.9727	0.90	0.82	8.81
	113	1.89	0.96	0.9733	0.96	0.87	9.75
P2	91	2.12	1.19	0.9819	0.92	0.94	2.17
	96	2.33	0.85	0.9782	1.07	1.11	3.74
	101	2.46	0.72	0.9815	1.14	1.15	0.01
	106	2.57	0.44	0.9762	1.38	1.41	2.17
P3	89	2.24	0.66	0.9975	1.20	1.21	3.77
	94	2.61	0.40	0.9869	1.42	1.47	2.25
	99	2.77	0.27	0.9771	1.61	1.65	4.63
	104	2.90	0.18	0.9848	1.82	1.90	4.62

Table 5. Active energy and crystallization parameters of samples

Polymer	ΔE (kJ/mol)	T_g (K)	$K_g \times 10^{-5}$ (K^2)	lnG_0
S0	-676.24	319.85	3.37	14.75
S1	-471.99	310.65	1.67	7.09
S2	-248.84	306.05	1.44	6.65
S3	-243.69	301.35	1.41	7.30

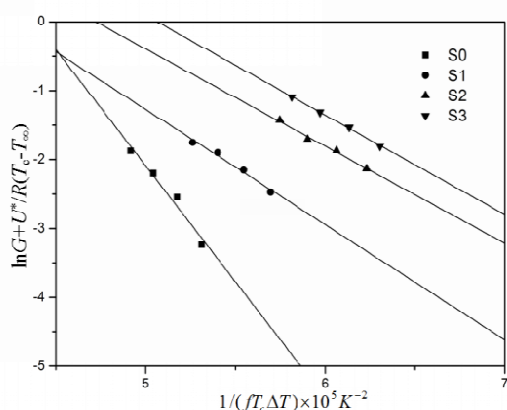indicating that the addition of nylon nylon-510 decreases the crystallization rate of copolymer [21].

Fig. 8. Plots of ln G + U*/[R(Tc -T∞)] versus 1/[fTc ΔT] for S0，S1，S2, and S3

3.7 Wide-Angle X-Ray Diffraction (WAXD)

Fig. 9 shows the WAXD profiles of S0~S3. As shown in Fig. 8, the WAXD data of S3 shows two strong reflections at 2θ values of 20.30 and 21.34°. When X_m increases from 0 to 15 mol%, the full width at half maximum (FWHM) and the height of diffraction decreases from 0.507 to 0.390 and 16373 to 13619, respectively. The peaks of the samples become weaker and the crystal zone become smaller. At the same time, the strong reflections at 2θ=20.30 gradually appear. What is more, the decrease in crystallinity of samples also can be obtained confirmed by WAXD results. The above results maybe because that the addition of nylon-510 disturbs the regularity of copolyamides molecular chain and results in the retard of crystallization rate [22-24].
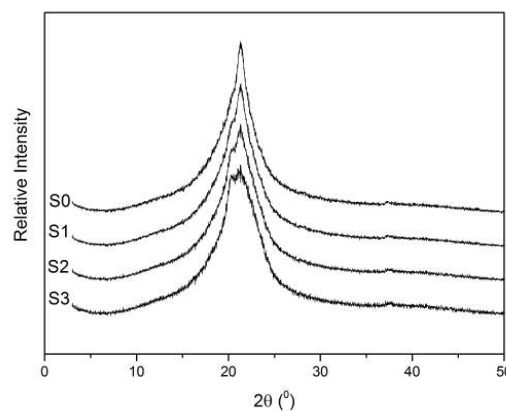

Fig. 9. Wide-angle X-ray spectra of S0, S1, S2, and S3

4. CONCLUSIONS

The samples of nylon 6/66 and nylon 6/66/510 containing 5 ~ 15 mol % nylon-510 were synthesized, and the isothermal crystallization kinetics and melting behaviors after isothermal crystallization of copolymer were systematically studied and the results showed that: (1) Avrami model can be used to describe the isothermal crystallization behavior of the copolyamides, and all the values of $t_{1/2}$ increase with increasing the T_c or the mole fraction of nylon 510. (2) The crystallization activation energy (ΔE) and nucleation constant (K_g) both increase with increasing the mole fraction of nylon-510, indicating that the addition of nylon-510 decreases the crystallization rate of copolymer.

COMPETING INTERESTS

Authors have declared that no competing interests exist.

REFERENCES

1. Sheng X, Lin Y. Monomer casting nylon-b-polymerher amine copolymers: Synthesis and properties. Composites Part B. 2015; 79:170-181.
2. Young TH, Lin DJ, Gau JJ, Chuan WY, Cheng LP. Morphology of crystalline Nylon-610 membranes prepared by the immersion precipitation process: Competition between crystallization and liquid-liquid phase separation. Polym. J. 1999;40:5011-5021.
3. Majed R, Sandra B, Nasreddine K, Nicolas D, Fabrice B, Caroline B, Marie HR, Corinne LB, Laurence L. Synthesis and physicochemical properties of new fatty (co)polyamides as potential UV powder coating. Prog. Org. Coat. 2015;87:171-178.
4. Octavie OD, Richard E, Verdu J, Fermagut F, Guilment J, Fayolle B. Molecular and macromolecular structure changes in polyamide 11 during thermal oxidation-kinetic modeling. Polym. Degrad. Stab. 2015;120:76-87.
5. Jin XD, Hu GS, Yang YF, Zhou XM, Wang BB. Nylon 6/66/11 copolymer used for hot-melt adhesives: Synthesis and properties. Int J. J. Adhes. Sci. Technol. 2009; 23(5):779-785.
6. Gerhard P, Jurgen S, Eberhard K. Low-melting copolyamide and their use as hot-melt adhesives. US patent. 2002;6:590:063.
7. Xiao XL, Zeng ZX, Xue WL, Kong QJ, Zhu WY. Isothermal crystallization kinetics and melting behaviors of poly(butylene terephthalate) and poly(butylene terephthalate-co-fumarate) copolymer. Int J. Polym. Eng. Sci. 2013;482-490.
8. Zeng ZX, Zhang HL, Xue WL, Zhu WY, Xiao XL, Sun Y, Li ZL. Isothermal crystallization kinetics of poly(butylene terphalate-co-sebacate) copolymer. J. Appl. Polym. Sci. 2011;121:735-742
9. Rewi SP, Tsen YC, Chiu KC, Chang SM, Chen YM. The crystallization kinetics of nylon 6/6T and nylon 66/6T copolymers. Thermochim Acta. 2013;555:37-45.
10. Huang Y, Li WH, Yan DY. Crystalline transition behaviors of nylons 12 20 and 10 20. Eur. Polym. J. 2003;39:1133-1140.
11. Wan JD, Li C, Fan H, Bu ZY, LI BG. Elucidating isothermal crystallization behaviors of nylon-11s. Influence star-chain branching. Thermochim Acta. 2013; 544:99-104.
12. Zhao ZD, Yu WX, Liu HH, Zhang JQ, Shao ZJ. Isothermal crystallization behaviors of nylon-6 and nylon-6/montmorillonite nanocomposite. Mater. Lett. 2004;58:802-806.
13. Shi JS, Yang XJ, Wang X, Lu LD. Non-isothermal crystallization kinetics of nylon 6/attpulgite nanocomposites. Polym. Test. 2010;29:596-602.
14. Hoffman JD. Regime III crystallizaition in melt-crystallized polymers: The variable cluster model of chain folding. Polymer. 1989;24:3-26.
15. He M, Zong SQ, Zhou YH, Guo HB, Fan QC. Non-isothermal crystallization kinetics of reactive microgel/nylon 6 blends. Chin. J. Chem. Eng. 2015;23:1403-1407.
16. Avrami M. Kinetics of phase change. I general theory. J. Chem. Phys. 1939;7: 1103-1112.
17. Avrami M. Kinetics of phase change. II transformation time relations for random distribution of nuclei. J. Chem. Phys. 1940;8:212-224.
18. Lin JX, Wang CY, Zheng YY. Prediction of isothermal crystallization parameters in monomer cast nylon 6. Comput. Chem Eng. 2008;32:3023-3029.
19. Reuvers NJW, Huinink HP, Adan OCG. Plasticization lags behind water migration in nylon-6: an NMR imaging and relaxation study. Polym. J. 2015;63:127-133.

20. Hoffman JD, Weeks JJ. Regime III crystallizaition in melt-crystallized polymers: The variable cluster model of chain folding. J. Res. Natl. Bur. Stand. Sect. A. 1962;66:13-28.

21. Zhou Q, Fang JH, Gao HQ, Loo LS. Substrate effects on the surface properties of nylon 6. Appl. Surf. Sci. 2013;282:115-120

22. Manci L, Osman RFM, Costa AMLM, Jose RM. Thermal and mechanical properties of polyamide 11 based composites reinfouced with surface modified titanate nanotubes. Mater. DES. 2015;83:459-467.

23. Men YF, Jens R. Temperature dependent wide angle X-ray diffraction studies on the crystalline transition in water saturated and dry polyamide 6/66 copolymer. Eur. Polym. J. 2004;40:2629-2635.

24. Kadam P, Vaidya P, Mhaske S. Synthesis and characterization of polyesteramide based hot melt adhesive obtained with dimer acid, castor oil and ethylenediamine. Int. J. Adhes. Adhes. 2014;50:151-156.

_____